Structural and electronic properties of hexagonal yttrium trihydride

Yan Wang and M. Y. Chou
School of Physics, Georgia Institute of Technology, Atlanta, Georgia 30332-0430
(Received 24 October 1994)

The structural and electronic properties of yttrium trihydride with metal atoms in the hexagonal-close-packed (hcp) structure are studied by the pseudopotential method within the local-density-functional approximation (LDA). It is found that the hydrogen positions within the metal lattice have a major role in determining these properties. Calculations confirmed that hexagonal YH_3 with unusual wavelike hydrogen displacements (space group D_{3d}^4 or $P\bar{3}c1$) is energetically more stable than the cubic structure. This result is consistent with neutron-diffraction data for YD_3 and for a heavy rare-earth trihydride HoD_3. These hydrogen displacements are identified as Peierls-like distortions in this three-dimensional system. The calculated final LDA band structure for YH_3 gives a semimetal rather than a semiconductor. With electron and hole pockets overlapping around the Γ point, the system is highly unstable. Other possible symmetry-breaking-distortion and many-body effects such as excitonic condensation are discussed.

I. INTRODUCTION

Yttrium hydrides have many characteristic properties in common with the hydrides of heavy rare-earth metals (Gd, Tb, Dy, Ho, Er, Tm, and Lu).[1] These systems have the largest possible hydrogen-to-metal ratio (up to 3) among elements. Their dihydrides are of the almost ideal cubic CaF_2-type structure in which the tetrahedral sites of a face-centered-cubic (fcc) metal lattice are filled by hydrogen. When the trihydride is formed, a structural transition occurs. The system goes to the hexagonal HoD_3-type structure instead of the cubic BiF_3-type structure (as in the case of light rare-earth trihydrides). While x-ray diffraction studies[2,3] concluded that the metal ions are in the hexagonal-close-packed (hcp) arrangement, neutron-diffraction results on HoD_3 (Ref. 4) and later on YD_3 (Refs. 5 and 6) revealed some unexpected displacements for the deuteron atoms. The unit cell was found to be three times larger than the conventional hcp unit cell with a $(\sqrt{3}\times\sqrt{3})R30^\circ$ expansion in the ab plane. Most interestingly, all hydrogen atoms are displaced away from ideal interstitial positions and exhibit a certain wave pattern. The octahedral hydrogen moves to new sites near the metal planes with additional wavelike vertical displacements. The tetrahedral hydrogen is also displaced from their original high-symmetry positions. This behavior is unique in yttrium and heavy rare-earth trihydrides and, to our knowledge, has never been seen in other metal-hydrogen systems. Previous researchers speculated that these unusual displacements are necessary to provide the required space for hydrogen.[4] As will be shown in this study, we find this behavior to be closely connected to the system's electronic structure.

For yttrium and heavy rare earths, the dihydride has metallic properties which gradually disappear as the hydrogen content approaches the trihydride composition. X-ray photoemission spectroscopy for YH_3 (Ref. 7) reveals a nearly symmetric core-level spectrum and weak emission at the Fermi level, which is consistent with the features of a semimetal or a semiconductor. Theoretical investigations of rare-earth systems are complicated by the presence of f electrons. Therefore the yttrium-hydrogen system would be the natural choice since it has no f states present near the Fermi level. The calculated properties of yttrium trihydride can probably be generalized to other systems in this group. These systems inspire several intriguing questions. Why does the metal lattice change back to its elemental structure (hcp) after a transition to the fcc structure in the dihydride phase? What causes the unique hydrogen displacements as observed in neutron diffraction studies?[4–6] How is the electronic structure affected by the displacement of hydrogen?

In this study, first-principles total-energy calculations are carried out in order to understand the peculiar phenomena in these metal trihydrides. Our calculations employ the pseudopotential method within the local-density-functional approximation (LDA).[8] By minimizing the total energy, the hydrogen positions within the lattice are determined. Some of the preliminary results have been published previously.[9] This paper presents the complete details of the calculation and summaries our study. For YH_3 the HoD_3-type structure is found to be energetically more stable than the cubic structure, consistent with experimental results. The arrangements of hydrogen atoms in the metal lattice play an important role in stabilizing the hexagonal phase. The predicted lattice constants a and c are in good agreement with experimental values. In addition, the structural transformation of the hydrogen sublattice is identified as a Peierls-like distortion resulting from special features in the electronic structure. With the remaining electron and hole bands crossing near the Fermi level, the LDA calculation yields a semimetal. (The electronic structure we obtained agrees with that from a recent calculation carried out independently by Dekker *et al.*[10] using the augmented-spherical-wave method.) However, the sys-

0163-1829/95/51(12)/7500(8)/$06.00

tem's unique electronic structure may lead to other electronic instability.

The paper is organized as follows. Section II describes general calculational techniques. The results and discussions are given in Sec. III, which is divided into three parts. Section III A is a detailed study of YH_3 in a conventional hcp unit cell. The total energies of different hydrogen configurations are investigated, and phase stability is examined and explained by analyzing the electronic structure and individual total energy terms. Section III B examines the structural distortions of the hydrogen sublattice and the resulting electronic structure. These displacements come from a Peierls-type lattice instability, the system's unusual electronic structure explaining the results. In Sec. III C, with the final electron and hole pockets centered at Γ, other possible atomic distortion and electronic instability are examined, including the possibility of an excitonic condensation in semimetallic YH_3. Section IV is the conclusion of this study.

II. CALCULATIONAL DETAILS

In the trihydride phase, the yttrium atoms form a hexagonal close-packed lattice. The experimentally measured lattice constants[4] for YH_3 are $a_0 = 3.672$ Å and $c_0 = 1.81a_0$. Compared with elemental yttrium, YH_3 has a lattice expansion of 0.6% and 15.9% in a_0 and the c_0/a_0 ratio, respectively, showing a large elongation along the hexagonal c axis ($c_0/a_0 = 1.57$ in elemental yttrium). The primitive cell used in the calculation has two in-plane lattice vectors forming an angle of 60° and the third one perpendicular to the plane. The origin is chosen at an octahedral site in order to make use of the system's inversion symmetry. This unit cell contains two yttrium atoms at $\pm(1/3, 1/3, 1/4)$, two octahedral interstitial sites at (0, 0, 0) and (0, 0, 1/2), and four tetrahedral interstitial sites at $\pm(1/3, 1/3, -1/8)$ and $\pm(1/3, 1/3, 5/8)$. They are all in units of primitive translational vectors. The octahedral sites are located halfway between the metal planes at a distance of $c_0/4$ from the planes. The ideal nearest-neighbor tetrahedral sites also have a separation of $c_0/4$. A metal atom is at a smaller distance to the nearest (perfect) T sites ($0.375c_0$) than to the nearest O sites ($0.405c_0$). Conventionally, hydrogen atoms are expected to occupy all the available interstitial sites to form a trihydride.

We carried out LDA calculations for YH_3 by using *ab initio* pseudopotentials with the Wigner correlation.[11] The wave functions are expanded with the plane-wave basis. Soft pseudopotentials were generated for both Y and H atoms.[12] The true $1/r$ ionic hydrogen potential is avoided here due to its poor convergence behavior. The hydrogen pseudopotential is generated from the atomic configuration $1s^1$, with a radial cutoff of 0.88 a.u., while the details of the yttrium potential have been reported elsewhere.[13] We tested the computational methods by studying the structural properties of elemental yttrium and the results are satisfying.[13] Good convergence is obtained with an energy cutoff of 30–40 Ry. This small energy cutoff value makes it feasible to perform supercell calculations later.

The total energies were obtained self-consistently with the eigenvalue problem solved by an iterative scheme. It took four to six iterations in order to achieve a good convergence (the total energy is stable to within 10^{-5} Ry). A total of 36 special k points were generated within the irreducible Brillouin zone for the single cell YH_3 calculation. In the calculation for the tripled cell with a smaller Brillouin and a larger matrix, the number used was largely reduced to 6. A Gaussian smearing method[14] was employed to accelerate the convergence of the total energy with respect to the number of k points. The energy difference between the two k-point sets was estimated to be within 10 meV per YH_3. We used about 2000 (6000) plane waves for the single (triple) cell calculations. The density of states (DOS) was obtained by using the tetrahedral method with 81 uniformly distributed k points in the irreducible Brillouin zone. Throughout the calculations, the experimental lattice constants[4] of both a_0 and c_0 were used for the hcp phase unless otherwise noted.

III. RESULTS AND DISCUSSIONS

A. YH_3 in a single hcp unit cell

We first investigated phase stability of yttrium trihydride in a single hcp unit cell. This cell can accommodate up to six hydrogen atoms by filling all the available interstitial sites, yielding a stoichiometric configuration of Y_2H_6 per cell. We will refer to the hydrogen occupying tetrahedral sites as H(T) and to those occupying octahedral sites as H(O). The energies for various atomic arrangements were calculated, with the binding energy per YH_3 defined as

$$E_b = E(YH_3) - E(Y_{\text{bulk}}) - 3E(H_{\text{atom}}), \qquad (1)$$

where $E(Y_{\text{bulk}})$ and $E(H_{\text{atom}})$ are the energy per atom for bulk yttrium and atomic hydrogen,[15] respectively. The results are listed in Table I for different hydrogen positions. These energies are compared with the equilibrium energy of cubic YH_3 where the metal atoms form an fcc lattice.

First, the ideal atomic arrangement was constructed with hydrogen occupying high-symmetry octahedral and tetrahedral sites. The calculated energy [(1) in Table I] was high, exceeding even that of the cubic phase. One would immediately ascribe this high energy to the fact that the nearest-neighbor tetrahedral hydrogens were too close together. Their separation of only 1.66 Å was too small according to the Switendick criterion.[16] We verified this by increasing the nearest-neighbor H(T)-H(T) pair distances. The optimal separation increased from the original separation of $0.25c_0$ to $0.3c_0$. This relaxation decreased the energy by 180 meV [(2) in Table I], but still yielded a higher energy than the cubic phase by 610 meV per YH_3. A lower energy configuration was found when all the octahedral hydrogen was uniformly shifted by $c_0/4$ along the c axis to the metal plane. [At the same

TABLE I. List of binding energies per YH_3 as defined in Eq. (1) for different hydrogen arrangements in a single hcp cell. Three hydrogen configurations are considered: (1) ideal tetrahedral and octahedral site occupation, (2) H(T) relaxed, and (3) H(T) relaxed and H(O) shifted to H(M). See the text for detailed explanations of each configuration.

Configurations	Binding energy (eV)	Difference (eV)
YH_3 (fcc)	−7.89	0
YH_3 (hcp)		
(1)	−7.10	+0.79
(2)	−7.28	+0.61
(3)	−8.08	−0.19

time, the separation of the nearest-neighbor H(T)-H(T) distance was kept at the optimal $0.3c_0$.] We will denote the hydrogen transferred from octahedral sites to metal planes as H(M). After this displacement, the distance between a metal atom and the closest hydrogen is much reduced. H(M) has three nearest-neighbor metal atoms at a smaller distance ($0.317c_0$) away than H(T) ($0.350c_0$). It resulted in a big drop in energy [(3) in Table I], about 0.98 eV per YH_3 lower than the ideal phase (1). Compared with cubic YH_3, the energy is lower by 190 meV per YH_3.

Clearly, the arrangement of hydrogen inside the hcp metal lattice plays an important role in determining phase stability of hexagonal yttrium trihydride. The theoretical values of equilibrium structural parameters, both the volume and the c_0/a_0 ratio, were checked for hydrogen configuration (3) by calculating and minimizing the total energies for different volumes and c_0/a_0 ratios. The calculated volume and c_0/a_0 ratio were 518 a.u. (Ref. 3) and 1.78, respectively, which were both within 2% of observed values. The high elongation along the hexagonal c axis mainly results from minimizing the strong repulsive interaction between nearest-neighbor H(T)-H(T) pairs.

One can understand the energy change better by analyzing individual energy contributions to the total energy as the positions of hydrogen are rearranged inside the hcp metal lattice [configurations (1), (2), and (3) above]. As expected, the increase in distance between nearest-neighbor H(T) pairs [from configuration (1) to (2)] lowered the kinetic and the core-core Coulomb (Ewald) energies. However, this is compensated partly by the electron-ion interaction energy since this off-center position reduced the interaction with metal atoms. When H(O) was moved down to the metal plane [from configuration (2) to (3)], a significant energy decrease came from the band energy term, primarily from the electron-ion interaction energy. Since the distance between the closest yttrium and hydrogen shrank, the Ewald energy also increased noticeably. The final balance between them led to a lower total energy for configuration (3). The lowering of the band energy is clearly the driving force for H(O) to move to the metal plane to stabilize the hexagonal structure.

The band dispersions along high-symmetry directions of the hcp Brillouin zone were calculated and compared for all three configurations with different hydrogen arrangements. Figures 1 and 2 show the dispersion curves of configurations (2) and (3), respectively. Comparing Figs. 1 and 2 shows that the Fermi energy decreased by 0.8 eV due to the transition from H(O) to H(M). This came from the significant lowering of certain bands across the Fermi level. One specific band is associated with the fourth state at Γ (Γ_1^+) which consists of a combination of H(M) s and yttrium $3z^2$-r^2 orbitals at Γ (see Fig. 2). The stronger hybridization between H(M) s and yttrium d electrons lowers its energy significantly. The wave-function decompositions of some selected states around the Fermi level at Γ and K are listed in Table II for configuration (3). Due to the change in the potential, the state K_2 with a majority d-like character was also pulled down below the Fermi level in Fig. 2. It consists of equally distributed xz and yz components (Table II) due to symmetry. As a result, the total band energy decreases substantially as mentioned above.

Another interesting feature in Fig. 2 is the existence of electron and hole pieces. The electron pocket, almost isotropic, is centered at K, while two coaxial hole pieces are present around the central axis of the Brillouin zone (from Γ to A). If the energy dispersion of the electron band is least-square fitted to a function $E = \beta[1-\cos(\alpha q)]$ along three independent directions K-Γ, K-H, and K-M, the effective masses at K from the fit are $0.35m$, $0.33m$, and $0.30m$, respectively (m is the mass of an electron). The inner hole surface is almost cylindrical, while the outer one is of the cigar shape with the radius ratio for the cross sections at $k_z = 0$ and $k_z = \pi/c_0$ planes close to two. The energy overlap between the electron and hole bands is about 1.34 (1.44) eV for the inner (outer) hole piece. The cross section of the Fermi surface at $k_z = 0$ is shown in Fig. 3, the vector $\mathbf{Q}$ (from Γ to K) connecting the centers of the electron and hole pieces. If the system's symmetry can be lowered and the electron and hole bands brought together via Brillouin-zone folding, they will cross each other near the Fermi level and a gap is likely to develop in order to lower the system energy. Depending upon the strength of the electron-

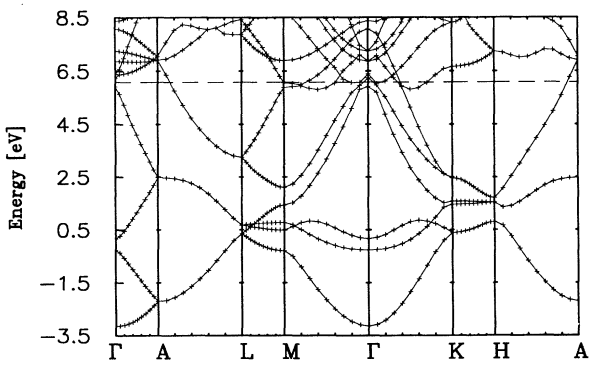

FIG. 1. Electronic bands of configuration (2) (see the text) with H(O) in their symmetry position and nearest-neighbor H(T) relaxed.

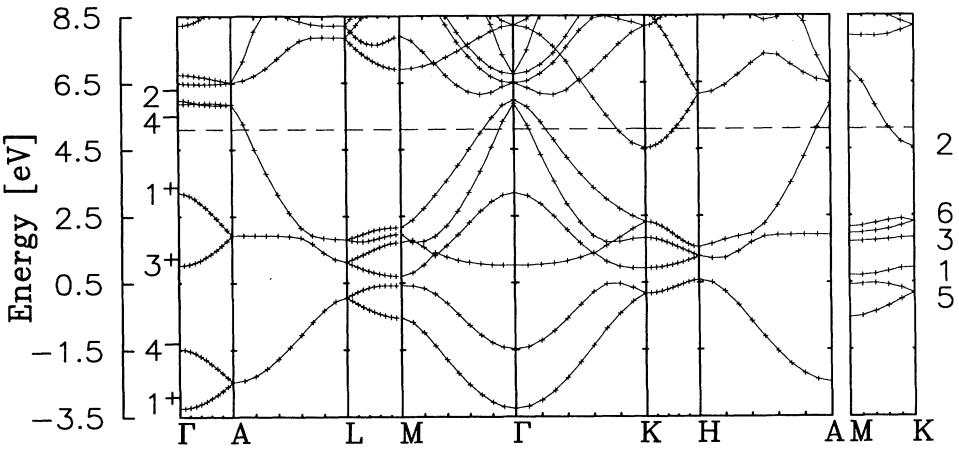

FIG. 2. Electronic bands of configuration (3) (see the text) with H(M) on the metal plane and nearest-neighbor H(T) relaxed.

phonon coupling,[17] some permanent symmetry-breaking atomic displacement similar to a Peierls distortion may be favored. We will investigate this lattice instability in the following subsection.

B. YH_3 with wavelike H displacements

As we have mentioned earlier in the paper, hydrogen positions in HoD_3 and YD_3 were studied by neutron diffraction.[4–6] Hydrogen arrangements in trihydrides of other hexagonal rare earths were speculated to be of a similar form. The HoD_3-type structure has a stacking sequence $ABAB\ldots$ with each stacking unit (A or B) consisting of three atomic groups: one layer of metal atoms and associated H(M), and two adjacent layers of H(T) (relaxed) above and below, respectively. Figure 3 shows the geometry of these three layers in one stacking unit: H(T) layers are shown in Figs. 3(a) and 3(c), where arrows indicate (small) horizontal displacements from ideal high-symmetry positions; Fig. 3(b) shows the arrangement of metal atoms denoted by big open circles and H(M) atoms by filled ones. Not all the H(M) atoms are on the metal plane; 1/3 of them are at a distance Δ_M be-

TABLE II. Population analysis for selected states in configuration (3) (see text). H(M) and H(T) stand for the hydrogen on the metal plane and at the tetrahedral site (relaxed), respectively. The numbers in parentheses are the corresponding population integrated over the sphere of radius 2.60 a.u. (1.40 a.u.) around the Y (H) site. The relatively small population for K_2 may indicate that there is a fair amount of wave-function distribution outsite the integrated region.

	Y	H(M)	H(T)
Γ_1^+	$3z^2-r^2$ (0.13)	s (0.14)	s (0.03)
Γ_4^-		s (0.16)	s (0.08)
Γ_2^-			s (0.16)
K_2	xz (0.09)		
	yz (0.09)		

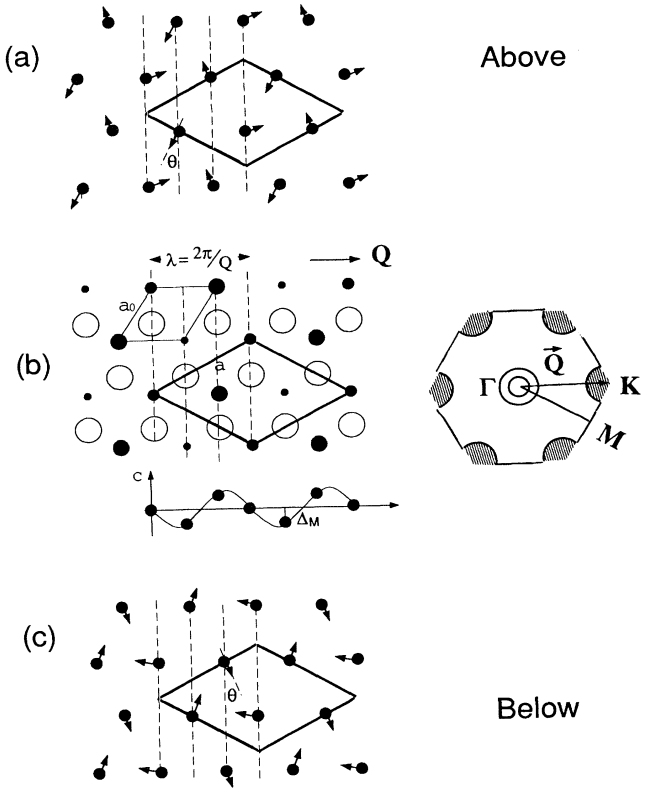

FIG. 3. Geometry of the three layers of a stacking unit in the HoD_3-type structure: (a) and (c) show, respectively, the upper and lower H(T) layers with arrows indicating the displacement of H(T); (b) shows the metal layer, which is composed of metal atoms denoted by big open circles and three types of H(M) which are above, on, and below the metal plane (denoted by large, medium, and small solid circles, respectively). The vertical modulation of H(M) is also displayed. The cross section of the enlarged unit cell is shown by thick lines, while the original single unit cell is shown by thin lines. The wavelength and wave vectors of the displacements are also shown, as well as the cross section of the Fermi surface for the bands in Fig. 2.

low (small filled circles) and 1/3 are at the same distance above (big filled circles), leaving only 1/3 on the plane. It is noted that the displacements of H(T) and H(M) are correlated and can be understood assuming a repulsive interaction between them. When an H(M) moves up (down) in Fig. 3(b), the three neighboring H(T) atoms in the layer below all move toward (away from) the central axis [see Fig. 3(c)]. The net displacement of H(T) makes an angle of θ from the symmetry line as indicated.

The vertical modulation of H(M) atoms plus the horizontal displacement of H(T) atoms form a three-dimensional frozen-in hydrogen displacement wave extending over the whole crystal. The wave vector **Q** and the wavelength $\lambda = 3a_0/2$ are given in Fig. 3. **Q** is exactly the vector from Γ to K in the Brillouin zone of the original hcp unit cell, which separates the electron and hole pockets in the undistorted structure. These distortions break the symmetry of the original hcp lattice (space group D^4_{6h}) and the new structure[4] can be described by the space group D^4_{3d} or $P\bar{3}c1$. As a consequence, the number of symmetry operations is reduced from the original 24 to 12 and the unit cell is enlarged by a factor of 3, as shown in Fig. 3(b). The new and old in-plane lattice vectors have a 30° rotation relative to each other, with the new lattice constants being $a = \sqrt{3}a_0$ and $c = c_0$ (a_0 and c_0 are the lattice parameters of the original hcp cell). This maps the original K points to the Γ point of the new Brillouin zone, causing the electron and hole pockets to be centered at the same point in the k space. Thus these wavelike hydrogen displacements are related to the special features of the electronic structure in Fig. 2.

We carried out total energy calculations for this triple-cell model with a stoichiometric composition of Y_6H_{18} per unit cell. As discussed earlier, there are two kinds of hydrogen displacements in the system: a vertical one for H(M) atoms (Δ_M) and a horizontal one for H(T) (Δ_T). [The H(T) rotation is first neglected.] The total energies are calculated on a two-dimensional mesh of Δ_M and Δ_T (assuming $\theta = 0$) and then fitted to a two-dimensional quadratic function. Figure 4 plots these energy values. We found the optimal displacements to be $\Delta_M = 0.055c$ (0.37 Å) and $\Delta_T = 0.017a$ (0.11 Å), with an energy lowering of 20 meV per YH_3. The magnitudes of these displacements are slightly different from

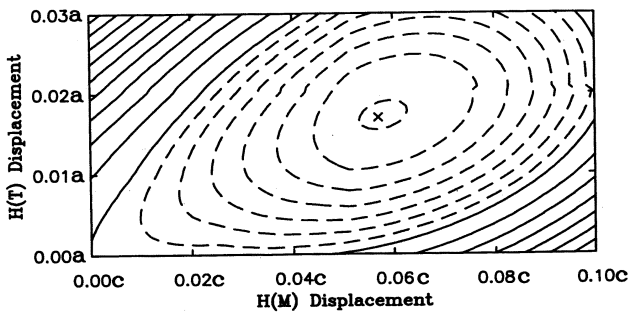

FIG. 4. Total energy contour plot as a function of displacements of H(M) and H(T). Dashed (solid) lines indicate lower (higher) energies than the undistorted structure.

experimental values.[4–6] For HoD_3 they are $\Delta_M = 0.083c$ and $\Delta_T = 0.026a$;[4] for YD_3, $\Delta_M = 0.083c$ and $\Delta_T = 0.030a$,[5] and $\Delta_M = 0.068c$ and $\Delta_T = 0.029a$.[6] We believe that the agreement is fair given the small energy variation involved. It is worth mentioning that one needs the correlated distortions of both H(T) and H(M) to lower the system energy; a single distortion alone was not sufficient.

Finally the angle θ (see Fig. 3) was varied while fixing Δ_M and Δ_T at the optimal values. The energy approaches a minimum at an angle roughly between 20° and 30°, with an energy decrease of about 10 meV per YH_3. Because of the energy curve's flatness near the minimum (< 1 meV over a 10° range) and the small energy difference comparable to the accuracy of the calculation, the optimal angle cannot be exactly determined (the zero point motion is likely to be important, which will be studied in future work on the system's dynamical properties.) One earlier refinement of YD_3 data[5] did not investigate the value for θ; the latest neutron study gave a value of 23°. The value for HoD_3 was about 10°.[4] Adding everything together, the final energy lowering resulting from these wavelike hydrogen displacements is about 30 meV per YH_3, which is small compared with the energy difference between the cubic and hexagonal phases found in Sec. III A, but large enough for us to confirm the existence of these displacements.

We also examined the change in electronic structure resulting from these hydrogen displacements. Figure 5(a) gives the band structure near the Fermi level along some symmetry directions for the system prior to any wavelike hydrogen displacements. It is the same dispersion as shown in Fig. 2, but folded to the smaller Brillouin zone of the triple cell. Two original K points $K^\alpha = (1/3, 2/3, 0)$ and $K^\beta = (2/3, 1/3, 0)$ (in terms of the reciprocal lattice vectors) are now mapped to the Γ point, resulting in a twofold degeneracy. The state K_2 right below the Fermi level in Fig. 2 now corresponds to a doubly degenerate state at Γ with Γ_1^- and Γ_2^+ symmetry. (We have followed the notation for the irreducible representations of the new space group D^4_{3d}.[18]) This band splits along the Γ-M direction, but is doubly degenerate in the other two directions shown. The hole pieces previously located along the Γ-A direction are unchanged. Their symmetry notations at Γ are now Γ_1^- and Γ_2^- (they were Γ_4^- and Γ_2^- in Fig. 2). The electron and hole bands cross near the Fermi level.

Figure 5(b) shows the energy bands of the system with $\Delta_T = 0$ and $\Delta_M = 0.05c$. Comparing Figs. 5(a) and 5(b) illustrates the dramatic effect of the transverse modulation of H(M) on the electronic structure. This displacement affects mostly the two bands associated with Γ_1^- (which originally cross each other) and opens a gap between them. The other two electron and hole bands (associated with Γ_2^+ and Γ_2^-) are not affected. Figure 5(c) shows the band structure at the optimal displacements of Δ_T and Δ_M with $\theta = 0$. The additional H(T) distortion further enhances the effect and both H(T) and H(M) displacements play an important role in this change. Figure 5(d) shows the band structure with the additional rotation of H(T) included. The result is similar to Fig. 5(c).

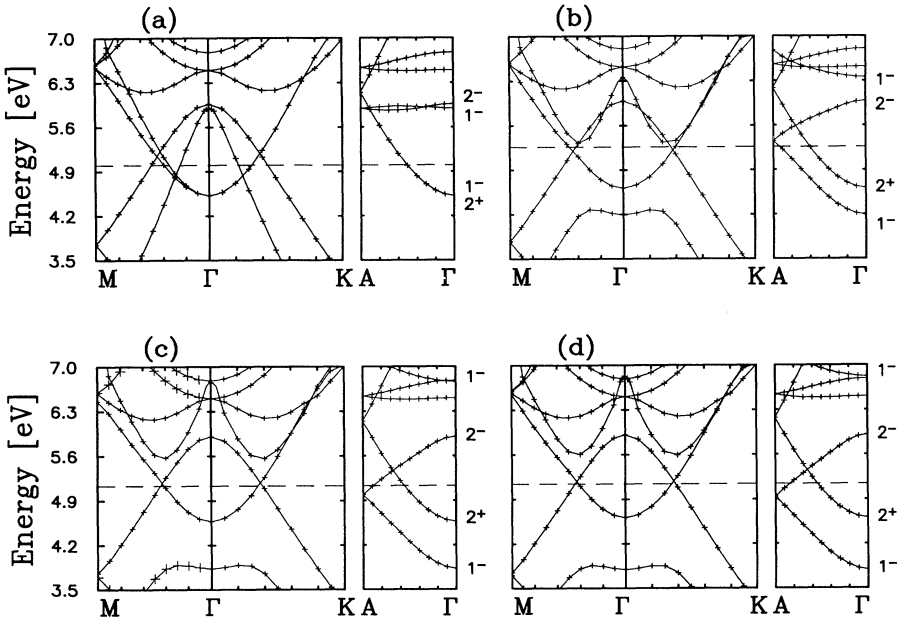

FIG. 5. Electronic structure for the triple cell cases: (a) H(O) hydrogens are in the metal plane; (b) H(O) hydrogens are shifted away from the metal plane, forming the wavelike modulation; (c) H(T) hydrogens move away from symmetry positions horizontally, while H(O) atoms remain shifted as in (b); (d) further rotational displacements for the H(T) hydrogens (see the text).

Two of the four bands near the Fermi level in Fig. 5(a) are now completely separated and the inner, cylindrically shaped hole pocket originally located along the Γ-A direction has vanished. The separation at the Γ point (Γ_1^-) of these two bands with the gap opened has increased from 1.38 eV to 3.03 eV. This change in the electronic structure gives rise to the small decrease in the total energy. There are still one electron band and one hole band remaining near the Fermi level.

We also analyzed the corresponding wave functions to understand the effect of these displacements on the electronic structure. As shown in Table II, the original K_2 states are composed of equal contributions of the xz and yz components of yttrium d orbitals. The wave functions at two different K points (K^α and K^β) have a different phase from each other. At $K^\alpha = (1/3, 2/3, 0)$,

$$f_\alpha = [(xz)_1 + (xz)_2] + i[(yz)_1 - (yz)_2] , \quad (2)$$

and at $K^\beta = (2/3, 1/3, 0)$,

$$f_\beta = [(xz)_1 + (xz)_2] - i[(yz)_1 - (yz)_2] , \quad (3)$$

where the subscripts 1 and 2 refer to the two yttrium atoms in the hcp unit cell. When these states are mapped to the Γ point for the enlarged unit cell, the wave functions of the doubly degenerate state will be linear combinations of these two functions. The one with the Γ_2^+ symmetry is made of $f_\alpha + f_\beta$, while the one with the Γ_1^- symmetry has $f_\alpha - f_\beta$. By symmetry the hydrogen displacements only affect the Γ_1^- state, not the Γ_2^+ state. Similar results were found for the two hole states at Γ where only Γ_1^- is affected, but not Γ_2^- [with H(T) s character].

Figure 6 shows the final DOS with all relaxations included. The eigenvalues are calculated for 81 special **k** points in the irreducible Brillouin zone of the triple cell. The calculated DOS is smoothed by the convolution of a Gaussian function with a width of 0.1 eV. The very small density of states at the Fermi energy, as well as the final band structure in Fig. 5(d), indicates that YH_3 is poorly metallic according to the LDA result. This conclusion is not in contradiction with the photoemission results,[7] which suggested this material be poorly metallic or semiconducting. We found a bandwidth of about 8 eV in the current calculation, which is smaller than the value calculated previously [about 9 eV (Ref. 19)] for fcc YH_3.

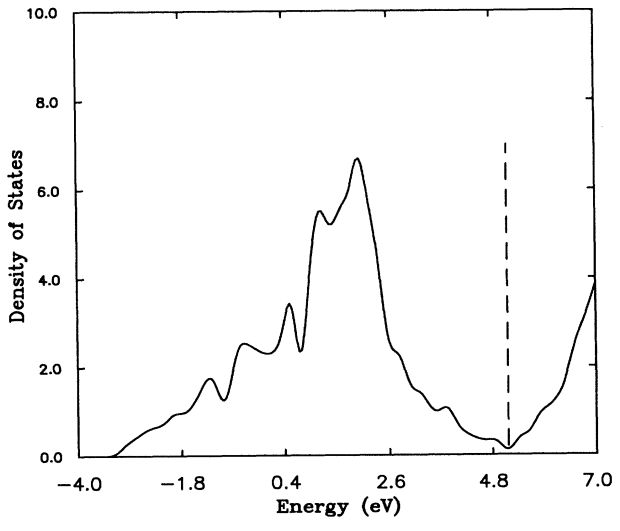

FIG. 6. Density of states for yttrium trihydride in the HoD_3 structure after considering all the relaxations. The calculated DOS has been convolved by a Gaussian function with a width of 0.1 eV.

C. Discussions

The final LDA band structure in Fig. 5(d) yields a compensated semimetal, with an electron band and a hole band, both nearly isotropic, overlapping around Γ. (The overlap is quite substantial, well beyond the LDA band energy uncertainties.) This is highly unstable electronically, since any mechanism that opens a gap will lower the electronic energy. We first examined the possibility of other hydrogen displacements. Since Γ_2^+ and Γ_2^- belong to different irreducible representations in the current space group D_{3d}^4, one possibility for them to interact in a lower-symmetry structure is to remove the inversion symmetry, namely, with the space group D_3^2 or $P321$. One possible atomic arrangement is to reverse the vertical displacement of H(M) in stacking units A and B with H(T) moved accordingly. This does not change the local environment within a stacking unit, but relative atomic positions between different layers of H(T) near the boundary of stacking units A and B are different. We carried out total energy calculations for this geometry and obtained a higher energy, about 20–50 meV per YH_3, for different amounts of displacements. Therefore removing inversion to further lower the symmetry is not energetically favorable. Refinements of recent neutron data[6] also indicated that the space group is D_{3d}^4.

The unusual band structure in Fig. 5(d) also leads one to speculate about other possible many-body effects. It has been predicted theoretically that under certain conditions the normal state consisting of Bloch waves in the crystal could become unstable against the spontaneous formation of excitons (electron-hole bound pairs).[20] It has been shown that if a semimetal has isotropic bands (coinciding electron and hole Fermi surfaces), the Coulomb interaction could cause this instability for any carrier density.[21,22] The same instability is also expected to occur in a semiconductor when the exciton binding energy exceeds the energy gap,[23] leading to a second-order phase transition to a new state having a condensate of excitons. In these cases the excitonic phase is always insulating. Depending on the strength of the electron-phonon coupling, the lowest energy state can exhibit spin-density waves or charge-density waves accompanied by a lattice distortion.[20] Interest in this subject has picked up after recent measurements of the Hall constant and resistivity of a narrow-gap semiconductor $TmSe_{0.45}Te_{0.55}$ under pressure provided evidence that this excitonic insulating phase exists.

In the final band structure of YH_3 shown in Fig. 5(d), the electron and hole energy bands are three dimensional and almost isotropic. The existence of these unusual overlapping electron and hole pockets and the similarity in size of the electron and hole Fermi surfaces seem to be what is required for an excitonic insulating ground state. The general parameters characterizing the semimetallic state of yttrium trihydride are list in Table III, where m^* is the averaged effective mass of electrons (or holes) obtained by a least-square fit to a quadratic function; n is the density of conduction electrons or holes; δE is the overlap between the top of the valence band and the bottom of the conduction band. If one keeps only the dominant term in the electron-electron interaction, the excitonic energy gap for a semimetal with isotropic bands is estimated to be[24]

TABLE III. List of parameters characterizing the semimetallic state of yttrium trihydride. m is the mass of the electron, n the electron (hole) density, and δE the band overlap.

YH_3	m^*	n (cm^{-3})	δE (eV)
	$0.4m$	5×10^{20}	1.30

$$\Delta_0 = 2\epsilon_F \exp\left(-\frac{1}{g}\right) \tag{4}$$

with

$$g = \frac{e^2 m^*}{\varepsilon \hbar p_F} \ln \frac{4p_F^2}{\hbar^2 \kappa^2}, \tag{5}$$

where κ is the reciprocal Debye screening radius, p_F is the Fermi momentum, ϵ_F is the Fermi energy, ε is the effective dielectric constant, and e is the electron charge. If the parameter values in Table III are used with the dielectric constant set to $\varepsilon = 10$ (5), Eq. (4) yields a gap of about 0.30 (0.46) eV. The gap equation has the form of the BCS gap equation in superconductivity and the thermodynamics of this transition are also analogous to that of the superconducting transition. Therefore the critical temperature T_g and Δ_0 follow the BCS relation

$$T_g = 0.28\Delta_0. \tag{6}$$

This would produce T_g around 1000 K for the energy gap estimated above.

In real YH_3 the bands are not perfectly isotropic and the electron and hole Fermi surfaces are not completely identical. This tends to lower the transition temperature or even suppress this instability. These will be the subject of future studies. The observed hydrogen displacements indicate the existence of charge-density waves, which may in turn be connected to the excitonic phase. Although no definitive connection can be made at the moment, it is noted that the anisotropy of the remaining hole pocket is greatly reduced after hydrogen displacements [see Figs. 5(a) and 5(d)], making the formation of the excitonic phase more favorable. Further experimental studies will be needed to resolve these issues.

IV. CONCLUSION

In summary, we have studied interesting properties of hexagonal yttrium trihydride from first-principles calculations. The calculated total energy for the HoD_3-type structure is lower than that for the cubic structure. We found that the major energy gain comes from lowering the band energy when the octahedral hydrogen moves to near the metal plane, which is quite an unusual position for

hydrogen in metal. We also found that additional hydrogen shifts off high-symmetry sites in the HoD_3 structure are frozen-in displacement waves, resulting from the sublattice instability in this three-dimensional system. It is closely connected to the system's electronic properties; the wave vector is exactly the vector separating the electron and hole pockets in the undistorted structure. The final density of states and electronic band structure from the LDA calculation indicate that YH_3 is a semimetal. We also examined other symmetry lowering distortions and could not find another structure that has a lower energy. With the remaining electron and hole bands centered at Γ and almost isotropic, an additional instability toward the excitonic insulating ground state is speculated. Assuming perfectly isotropic energy bands, the energy gap is estimated to be 0.3–0.4 eV and the transition temperature is around 1000 K. The actual anisotropy will affect the stability of this excitonic phase and will be the subject of future studies.

ACKNOWLEDGMENTS

We would like to thank Dr. A. C. Switendick, Dr. T. J. Udovic, and Dr. Q. Huang for general discussions. This work was supported by the U.S. Department of Energy under Contract No. DE-FG05-90ER45431 and partly by the NSF. A grant for supercomputer time from the Pittsburgh Supercomputing Center (DMR890007P) is also acknowledged. M.Y.C. thanks the Packard Foundation for their support.

[1] G. G. Libowitz and A. J. Mealand, in *Handbook on the Physics and Chemistry of Rare Earths,* edited by K. A. Gschneidner, Jr. and L. Eyring (North-Holland, Amsterdam, 1979), Vol. 3, p. 299.
[2] F. H. Spedding, A. H. Daane, and K. W. Herrmann, Acta Crystallogr. **9**, 559 (1956).
[3] A. Pebler and W. E. Wallace, J. Phys. Chem. **66**, 148 (1962).
[4] M. Mansmann and W. E. Wallace, J. Phys. (Paris) **25**, 454 (1964).
[5] N. F. Miron, V. I. Scherbak, V. N. Bykov, and V. A. Levdik, Kristallografiya **17**, 404 (1972) [Sov. Phys. Crystallogr. **17**, 342 (1972)].
[6] T. J. Udovic, Q. Huang, and J. J. Rush (unpublished).
[7] A. Fujimori and L. Schlapbach, J. Phys. C **17,** 341 (1984).
[8] P. Hohenberg and W. Kohn, Phys. Rev. **136**, B864 (1964); W. Kohn and L. J. Sham *ibid.* **140**, A1133 (1965).
[9] Y. Wang and M. Y. Chou, Phys. Rev. Lett. **71**, 1226 (1993).
[10] J. P. Dekker, J. van Ek, A. Lodder, and J. N. Huiberts, J. Phys. Condens. Matter **5**, 4805 (1993).
[11] E. Wigner, Phys. Rev. **46**, 1002 (1934).
[12] N. Troullier and J. L. Martins, Phys. Rev. B **43**, 1993 (1991).
[13] Yan Wang and M. Y. Chou, Phys. Rev. B **44**, 10 339 (1991).
[14] C. L. Fu and K. M. Ho, Phys. Rev. B **28**, 5480 (1983).
[15] The energy of atomic hydrogen (−13.6058 eV) is used as the reference. Using the supercell method and the same pseudopotential, we have done the calculation for H_2. The bond length is found to be 0.79 Å and the binding energy per hydrogen is 3.21 eV. Comparing with the experimental value of the bond length 0.74 Å and the binding energy per hydrogen 2.35 eV, our result overestimated the binding energy, as expected for LDA calculations. The cutoff of the core radius for H pseudopotential may introduce some core overlap when two H get as close as 0.79 Å in H_2. Therefore, we decided to use the energy of atomic hydrogen as the reference point for various binding energies.
[16] A. C. Switendick, Adv. Chem. Ser. (U.S.) **167**, 264 (1978).
[17] S. K. Chan and V. Heine, J. Phys. F **3**, 795 (1973).
[18] See, for example, T. Inui, Y. Tanabe, and Y. Onodera, *Group Theory and Its Applications in Physics* (Springer-Verlag, New York, 1990), p. 371.
[19] A. C. Switendick, J. Less-Common Met. **74** 199, 1980.
[20] For a review, see B. I. Halperin and T. M. Rice, in *Solid State Physics*, edited by F. Seitz, D. Turnbull, and H. Ehrenreich (Academic, New York, 1968), Vol. 21, p. 116.
[21] L. V. Keldysh and Yu. V. Kopaev, Fiz. Tverd. Tela (Leningrad) **6**, 2791 (1964) [Sov. Phys. Solid State **6**, 2219 (1965)].
[22] A. N. Kozlov and L. A. Maksimov, Zh. Eksp. Teor. Fiz. **48**, 1184 (1965) [Sov. Phys. JETP **21**, 790 (1965)].
[23] J. de Cloizeaux, J. Phys. Chem. Solids **26**, 259 (1965).
[24] Yu. V. Kopaev, Tr. Fiz. Instituta P.N. Lebed. **86**, 3 (1975).